Comprehensive Analysis and Reduction of Torque Ripples in Three-phase Four-switch Inverter-fed DFIG Drives Using Space Vector Pulse-width Modulation

Munendra Pratap Singh [1,] Dr. Pratibha Tiwari [2,]

Electrical Engineering from Sam Higginbottom Institute of Agriculture, Technology India and Sciences, Allahabad, Uttar Pradesh, India[1]

Electrical Engineering from Sam Higginbottom Institute of Agriculture, Technology and Sciences, Allahabad, Uttar Pradesh, India[2]

Abstract— As a result of their reduced number of switches, three-phase four-switch (TPFS) inverters are generally applied as cost-reduction topologies for. This paper deals with the operation of doubly fedinduction generator (DFIG) with an integrated active filter capabilities using grid-side converter (GSC). The main contribution of this work lies in the control of GSC for supplying harmonics in addition to its slip power transfer. The rotor-side converter (RSC) is used for attaining maximum power extraction and to supply required reactive power to DFIG, for supplying harmonics even when the wind turbine is in shutdown condition. Control algorithms of both GSC and RSC are presented in detail. However, the torque ripples of DFIGs severely deteriorate the performance and reliability of the entire system. Hence, comprehensive considerations for torque ripple reduction, including high- and low-frequency torque ripples, are elaborated considering TPFS inverter-fed DFIG drives. The second-order torque harmonics produced by DC capacitor voltage fluctuations are first demonstrated, and a very simple compensation method is presented by introducing a novel non-orthogonal coordinate transformation. Then, to evaluate the effects on the high-frequency torque ripples of space vector modulation (SVM) schemes, three SVM schemes for TPFS inverter-fed PMSM drives are assessed based on the torque ripple root mean square (RMS) value. Consequently, the preferred SVM scheme is obtained for high-frequency torque ripple minimization. Moreover, the linear modulation range of the TPFS inverter-fed DFIG drive is derived considering capacitor voltage fluctuations, therein avoiding the low-frequency torque ripples caused by over-modulation. Meanwhile, an adaptive capacitor voltage offset suppression method is proposed to fully exploit the DC link voltage. The proposed analysis and methods for torque ripple reduction. DFIG-based WECS is demonstrate the validation and effectiveness simulated using MATLAB/Simulink.

***Keywords*—Capacitor voltage fluctuation Doubly fed induction generator (DFIG), integrated active filter, nonlinear load, power quality,, space vector modulation (SVM), three-phase four-switch (TPFS) inverter, torque ripple reduction**

I. INTRODUCTION

PMSMs, driven by three-phase voltage-source inverters with six switches (TPSS), have become the central aspect of variable-frequency drive systems in many industrial applications because of their superior features such as their high efficiency and high power density. However, in certain applications, cost reduction of the inverter configuration is taken as the priority. Therefore, the three-phase four-switch (TPFS) inverter presented in [1]-[11] represents a promising option for replacing the TPSS inverters due to its reduced number of power switches. In addition, the TPFS inverter can be utilized to ride through open/short-circuit faults of the TPSS inverter, which is quite valuable in some critical applications, such as wind power generation [7], [8]. In PMSM drives, an inherent drawback to be inhibited is torque ripples, which cause undesirable acoustic noise and torsional vibrations, even resulting in shaft failures [12], [13]. Hence, several techniques for the torque ripple reduction are introduced to improve the performance of PMSM drives.

In[14]-[17], the cogging torque of a PMSM is suppressed using motor design techniques such as skewing, fractional slot pitch winding and optimized magnetic design. In [1]-[2], the pulsating torque caused by the back-EMF harmonics in the PMSM is compensated by active control methods, such as repetitive control, iterative learning control and self-adaptive control. Furthermore, as a prominent consequence of the nonsinusoidal voltages impressed by the converters, the high frequency torque harmonics in PMSMs are strongly influenced

by the adopted voltage vectors during the switching period [12], [13]. Therefore, [utilize additional active vectors and optimize their duration times during the switching period to reduce torque ripples in direct-torque-controlled (DTC) PMSM drives. However, torque ripple reduction methods are mainly focused on TPSS inverter-fed PMSM drives. Still, some other considerations for torque ripples remain to be applied to TPFS inverter-fed PMSM drives. In TPSS inverter-

fed PMSM drives, the neutral point voltage of the DC bus is constant, which has no effect on the torque performance. In contrast, in a TPFS inverter-fed PMSM drive, one phase of stator current directly flows into the midpoint of the DC split capacitors, resulting in periodical fluctuations of the capacitor voltages. However, the modulation techniques for TPFS inverters discussed in [1]-[11] ignore the capacitor voltage oscillations; thus, imbalanced stator currents are produced, resulting in pulsating torques. Moreover, due to the absence of zero vectors in the TPFS inverter, various equivalent zero vector synthesis approaches in the space vector modulation (SVM) are proposed in [1]-[11]. However, the effects on the high frequency torque harmonics of the zero vector synthesis methods have not been analyzed in detail.

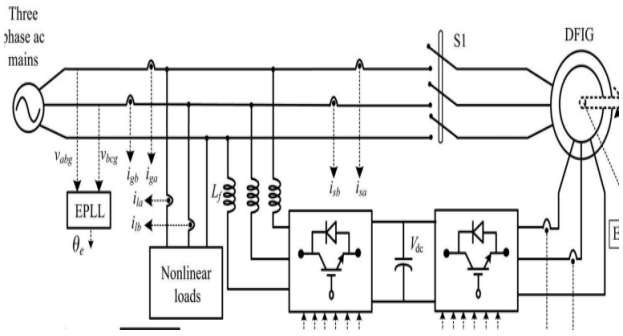

Fig. 1. Topology of the TPFS inverter-fed dfig drive

Therefore, an in-depth analysis of torque ripples influenced by the SVM strategies in a TPFS inverter-fed PMSM drive for reducing the high-frequency torque harmonics should be provided. In addition, the capacitor voltage fluctuations strongly impact the linear modulation range of the TPFS inverter, which has not been mentioned previously. If the capacitor voltage fluctuations are not considered, the TPFS inverter-fed PMSM drive may operate in the over-modulation zone with an improper DC bus voltage, thus producing abundant low-frequency torque harmonics. Meanwhile, the linear modulation range also deteriorates as a result of the DC offset of the two capacitor voltages, which should be eliminated. However, the capacitor voltage offset suppression method in [6] and [7] utilizes a second-order low pass filter (LPF) to extract the DC offset component, which is not applicable to TPFS inverter-fed PMSM drives under low-speed conditions due to the reduced stability margin of the control loop caused by the limited bandwidth of the LPF. Thus, an improved capacitor voltage offset suppression method applicable to TPFS inverter-fed PMSM drives is required to eliminate the low-frequency torque ripple caused by the limited linear modulation range.

In this study, the comprehensive analysis of torque ripple reduction is presented in terms of a TPFS inverter-fed DFIG drive, including the modulation scheme, the linear modulation range, and a suitable control strategy. The pulsating torque in the TPFS inverter-fed DFIG drive produced by the uncompensated modulation strategies is first illustrated, and a simple compensated method is proposed to directly obtain the duty ratios by introducing a novel coordinate transformation. Then, the influence on the high-frequency torque harmonics of the SVM strategies is analyzed by introducing the root mean square (RMS) value of the torque ripple. Additionally, three SVM strategies for TPFS inverter-fed PMSM drives are analytically evaluated in terms of their abilities to reduce the high-frequency torque ripples. Moreover, the linear modulation range of the TPFS inverter-fed PMSM drive is fully investigated considering capacitor voltage fluctuations. According to the proposed analysis, appropriate DC bus voltages under various operating conditions can be easily obtained to eliminate the low frequency torque ripple caused by over-modulation. Meanwhile, an adaptive DC offset voltage suppression method that is suitable for TPFS inverter-fed DFIG drives under any operating condition is proposed. Consequently, the DC bus voltage is fully exploited to eliminate the low-frequency torque ripple caused by the capacitor voltage offset. The experimental results show that the proposed analysis and methods for torque ripple reduction are valid and effective.

II. SYSTEM CONFIGURATION AND OPERATING PRINCIPLE

Fig. 1 shows a schematic diagram of the proposed DFIG based. WECS with integrated active filter capabilities. In DFIG, the stator is directly connected to the grid as shown in Fig. 1. Two back-to-back connected voltage source converters (VSCs)are placed between the rotor and the grid. Nonlinear loads are connected at PCC as shown in Fig. 1. The proposed DFIG works as an active filter in addition to the active power generation similar to normal DFIG. Harmonics generated by the nonlinear load connected at the PCC distort the PCC voltage.These nonlinear load harmonic currents are mitigated by GSC control, so that the stator and grid currents are harmonic-free. RSC is controlled for achieving maximum power point tracking (MPPT) and also for making unity power factor at the statorside using voltage-oriented reference frame. Synchronous reference frame (SRF) control method is used for extracting the fundamental component of load currents for the GSC control.

III. DESIGN OF DFIG-BASED WECS

Selection of ratings of VSCs and dc-link voltage is very much important for the successful operation of WECS. The ratings of DFIG and dc machine used in this experimental system are given in Appendix. In this section, a detailed design of VSCs and dc-link voltage is discussed for the experimental systemused in the laboratory.

a. Selection of DC-Link Voltage

Normally, the dc-link voltage of VSC must be greater than twice the peak of maximum phase voltage. The selection of

dclink voltage depends on both rotor voltage and PCC voltage. While considering from the rotor side, the rotor voltage is sliptimes the stator voltage. DFIG used in this prototype has stator to rotor turns ratio as 2:1. Normally, the DFIG operating slip is ±0.3. So, the rotor voltage is always less than the PCC voltage. So, the design criteria for the selection of dc-link voltage can be achieved by considering only PCC voltage. While considering

IV. CONTROL STRATEGY

Control algorithms for both GSC and RSC are presented in this section. Complete control schematic is given in Fig. 2. The control algorithm for emulating wind turbine characteristics using dc machine and Type A chopper is also shown in Fig. 2.

a. *Control of RSC*

The main purpose of RSC is to extract maximum power with independent control of active and reactive powers. Here, the RSC is controlled in voltage-oriented reference frame. Therefore, the active and reactive powers are controlled by controlling direct and quadrature axis rotor currents (*i*dr and *i*qr), respectively. Direct axis reference rotor current is selected such that maximum power is extracted for a particular wind speed. This can be achieved by running the DFIG at a rotor speed for a particular wind speed. Therefore, the outer loop is selected as a speed controller for achieving direct axis reference rotor current ($i*$ dr) as $i*\text{dr}(k) = i*\text{dr}(k-1) + k\text{pd}\{\omega\text{er}(k) - \omega\text{er}(k-1)\} + k\text{id}\omega\text{er}(k)$ (4) where the speed error (ωer) is obtained by subtracting sensed speed (ωr) from the reference speed ($\omega r*$). *k*pd and *k*id are the proportional and integral constants of the speed controller. $\omega\text{er}(k)$ and $\omega\text{er}(k-1)$ are the speed errors at *k*th and (*k*-1)th instants. $i*\text{dr}(k)$ and $i*\text{dr}(k-1)$ are the direct axis rotor reference current at *k*th and (*k*-1)th instants. Reference rotor speed ($\omega r*$) is estimated by optimal tip speed ratio control for a particular wind speed. With the parameters of the proposed TPFS inverter-fed PMSM drive listed in Table II, the minimum required DC voltage *VDCmin* for linear modulation is depicted in Fig. 9 and Fig. 10. Clearly, the *VDCmin* calculated using (43) is related to

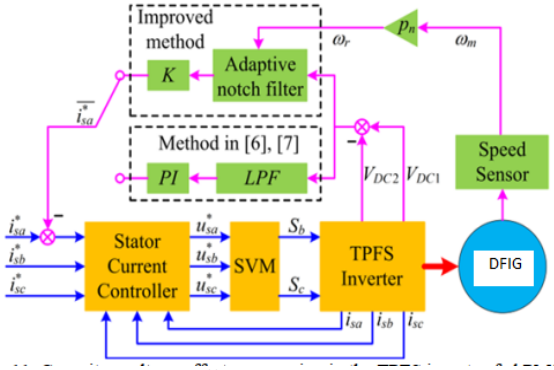

Fig. 11. Capacitor voltage offset suppression in the TPFS inverter-fed DFIG drive.

the electromagnetic torque *Te*, the capacitor voltage offset Δ*VDC* and the rotor speed ωm. In general, with increasing *Te*, the capacitor voltage fluctuation more severely deteriorates the linear modulation range, as seen from (38). Consequently, *VDCmin* increases with increasing *Te*, as shown in Fig. 9. Similarly, the capacitor voltage offset Δ*VDC* limits the full use of the DC bus voltage, which also deteriorates the linear modulation range of the TPFS inverter-fed PMSM drive. From Fig. 9 and Fig. 10, *VDCmin* increases linearly with increasing rotor speed ω_m in the high rotor speed zone mainly because the stator voltage magnitude increases linearly with ω_m, as depicted in (8). Nevertheless, when the rotational speed ω_m is low, the capacitor voltage fluctuation is also aggravated, as seen from (38). Consequently, as shown in Fig. 9 and Fig. 10, a high value of V_{DCmin} is required in the low rotational speed zone if takingcapacitor voltage fluctuations into account, which is not seen in the conventional over-modulation judgment with (36).

The proposed analysis provides sufficient insight into the linear modulation range of the TPFS inverter-fed DFIG drive, where the effects of the capacitor voltage fluctuations and offset arerevealed. Therefore, the low frequency torque ripples caused by the over-modulation can be avoided by selecting an appropriate DC link voltage with (43).As described above, the linear modulation range of the TPFS inverter-fed PMSM drive is deteriorated by the capacitor voltage offset. In practice, the dynamic behaviors of the DFIG, such as accelerating and decelerating, inject the DC component into the phase current, which produces the DC offset of the capacitor voltages.Thus, active control methods for suppressing the capacitor voltage offset are required to reduce torque ripples caused by the over-modulation.

VI. SIMULINK RESULTS

The Simulink setup of a TPFS inverter-fed DFIG test bench is depicted in Fig. 13. The control board of the Simulink setup is based on the 32-bit digital processor the TPFS inverter is the The DFIG used in the simulink test is a 2-kW, 8 pole pairs, surface-mounted DFIG whose rated speed is 40rpm. The load torque is provided by a PMSG connected to the same shaft of the tested DFIG. The rest parameters of the test bench are shown in Table II. In this study, the back EMFs of the PMSM are assumed to be pure sinusoidal and balanced to simplify the analysis. Therefore, the back EMF of the PMSM with no load are tested first at theconstant speed of ω_m=30 rpm to demonstrate the validity of the assumption. As shown in Fig. 14(a), it is clear that the back EMFs are almost perfect sinusoidal and balanced. The FFT analysis results of the back EMFs are also provided in Fig. 14 (b), which shows that there are little harmonic distortions in the back EMFs. Thus, the experimental results are well coincident with the above assumption, guaranteeing the effectiveness andvalidity of the analysis results.

A comparative study between the uncompensated compensated modulation strategy is developed, where T_e=200

Nm, ω_m=30 rpm and V_{DC}=400 V. It is worth noting that the adopted switching sequence has no effect on the duty ratios of the powerswitches, because they are only determined by whether the capacitor fluctuations are considered. Therefore, the NVSVM scheme is utilized in this test to present the effectiveness of the proposed compensated modulation strategy. As shown in Fig. 15, the stator currents are unbalanced when the uncompensated method is utilized, which is coincident with the analysis results in Section III. Also, a 2nd-order torque ripple is obvious whenusing the uncompensated modulation method, and the Fourier analysis results also demonstrate that there is a 2nd-order torque harmonic of 25 Nm in the DFIG drive. Using the compensated method, the 2nd-order torque ripple is alleviated, a result that is also supported by the Fourier analysis, as shown in Fig. 16. The experimental results imply that the capacitor voltage fluctuation cannot be ignored in the modulation method, eliminate the resultant 2nd-order torque ripple effectively.

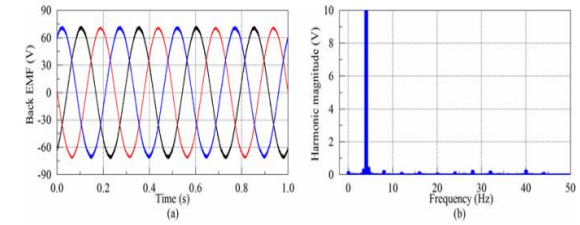

Fig. 14. Simulink l results of the back EMF at ωm=30 rpm.

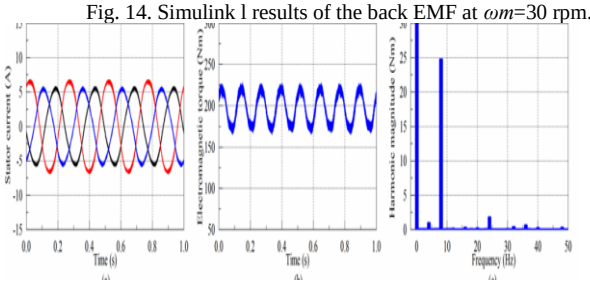

Fig. 15. Simulink results when using uncompensated modulation scheme with *VDC*=400 V, ωm=30 rpm and *Te*=200 Nm : (a) stator current; (b) torque; (c) FFT analysis result of the torque

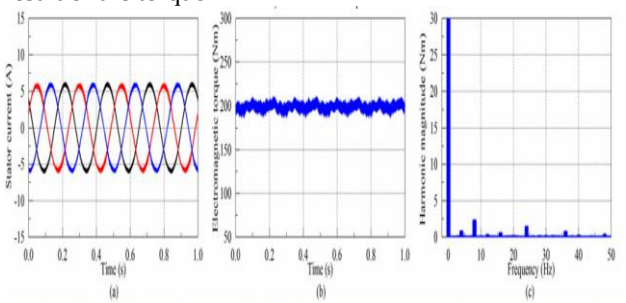

Fig. 16. Simulinkl results when using proposed compensated modulation scheme with VDC=400 V, ωm=30 rpm and Te=200 Nm: (a) stator current; (b) torque; (c) FFT analysis result of the torque.

The effects of the various SVM schemes on the torque ripple are also tested. The SVSVM, LVSVM and NVSVM are implemented in the experimental setup, with V_{DC}= 500 V, The linear modulation range of the TPFS inverter-fed DFIG drive is also tested under various operating conditions with the NVSVM method. The impact of torque on the linearmodulation range is studied first. In Fig. 16, the simulink results are obtained when the TPFS inverter-fed DFIGdrive operates at T_e=200 Nm, ω_m=30 rpm and V_{DC}=400 V, in which the torque is not distorted by low frequency harmonics. The simulink results not only show that the 2nd-order torque ripples are eliminated by the proposed compensated modulation strategy, but also demonstrate the TPFS inverter-fed DFIG drive operates in the linear modulation range at T_e=200 Nm, ω_m=30 rpm and V_{DC}=400 V. However,when the torque increases to 350 Nm,

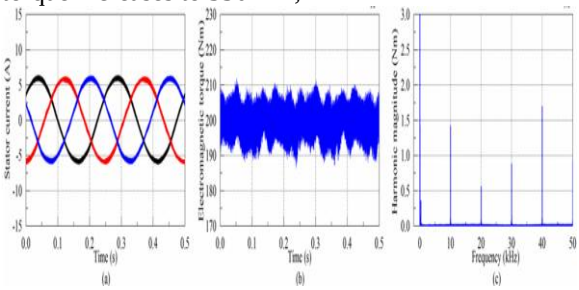

Fig. 17. Simulink result for the SVSVM with *VDC*=500 V, ωm=30 rpm and *Te*=200 Nm: (a) stator current; (b) torque; (c) FFT analysis result of the torque.

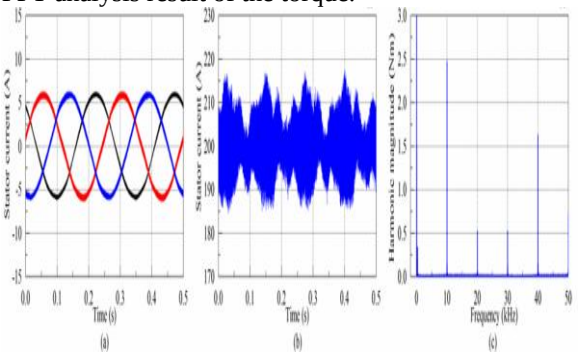

Fig. 18.Simulink result for the LVSVM with *VDC*=500 V, ωm=30 rpm and *Te*=200 Nm: (a) stator current; (b) torque; (c) FFT analysis result of the torque

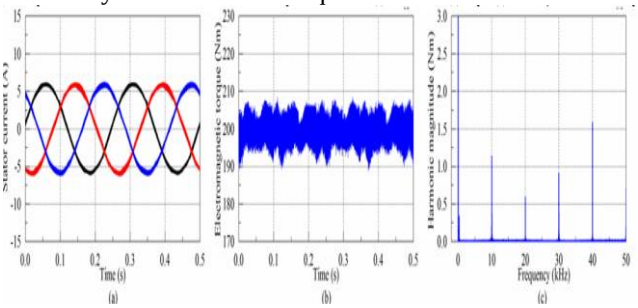

Fig. 19. Simulink result for the NVSVM with *VDC*=500 V, *ωm*=30 rpm and *Te*=200 Nm: (a) stator current; (b) torque; (c) FFT analysis result of the torque.

the TPFS inverter-fed DFIG drive operates beyond the linear modulation range according to (31). This theoretical analysis is supported by the torque ripples are produced by the increased torque; the FFT analysis also shows that the low-frequency torque harmonics are obviously increased by the over-modulation. To avoid the torque ripples caused by the over-modulation, the DC bus voltage V_{DC} is then set to 500 V according to (31). Thus, the low-frequency torque ripple is eliminated because the TPFS inverter-fed DFIG drive operates in the linear modulation range again, as shown in Fig. 22.

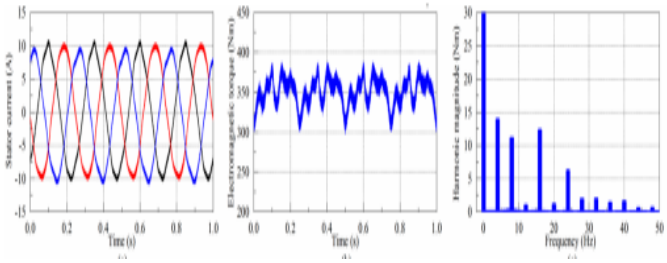

Fig. 21. Simulink results for the over-modulation range test with *VDC*=400 V, *ωm*=30 rpm and *Te*=350 Nm: (a) stator current; (b) torque; (c) FFT analysis result of the torque

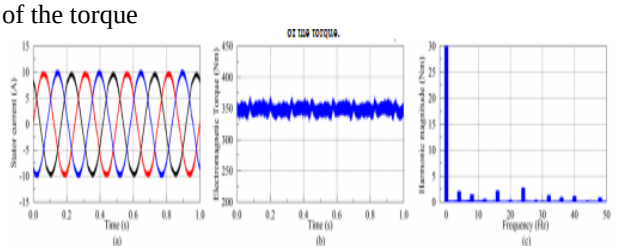

Fig. 22. Simulink results for the over-modulation range test with *VDC*=500 V, *ωm*=30 rpm and *Te*=350 Nm: (a) stator current; (b) torque; (c) FFT analysis result of the torque.

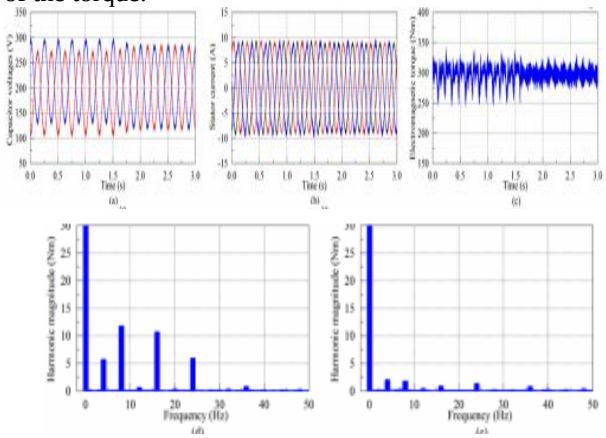

Fig. 23. Simulink results for the over-modulation range test with *VDC*=400 V, *ωm*=30 rpm and *Te*=300 Nm: (a) capacitor voltages; (b) stator current; (c) torque;(d) FFT analysis of the torque when Δ*VDC*=20 V; (e) FFT analysis of the torque when Δ*VDC*=0 V.

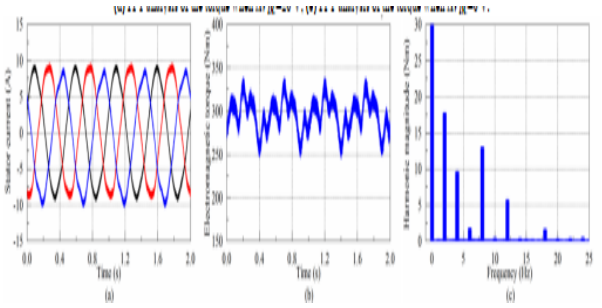

Fig. 24 Simulink results for the over-modulation range test with *VDC*=400 V, *ωm*=15 rpm and *Te*=300 Nm: (a) stator current; (b) torque; (c) FFT analysis result of the torque

.

The effects of the capacitor voltage offset on the linear modulation range are also tested. At V_{DC}=400 V, ω_m=30 rpm and T_e=300 Nm, the capacitor voltage offset ΔV_{DC} is initially equal to 20 V without the capacitor voltage offset control, as shown in Fig. 23(a). Thus, over-modulation occurs in the TPFS inverter-fed PMSM drive, resulting in undesirable low-frequency torque ripples, as shown in Fig. 23(c). The FFT analysis in Fig. 23(d) also proves that the capacitor voltage offset produces the low-frequency torque harmonics. With the implementation of the proposed capacitor voltage offset suppression method at *t*=1.5s, ΔV_{DC} is decreased to null, as seen in Fig. 23(a). Then, the over-modulation of the TPFS inverter-fed PMSM drive is avoided, where the low-frequency torque ripple is rejected, as shown in Fig. 23(c). Meanwhile, the FFT analysis in Fig. 23(e) also demonstrates that the low-frequency torque harmonics are reduced via the elimination of the capacitor voltage offset. The impact of the rotor speed ω_m is also tested. From Fig. 23, it is clear that the PMSM drive operates in the linear modulation range at V_{DC}=400 V, ω_m=30 rpm and T_e=300 Nm. However, (31)

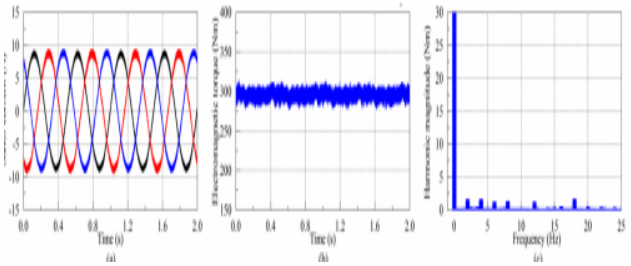

Fig. 25. Simulink results for the over-modulation range test with *VDC*=500 V, *ωm*=15 rpm and *Te*=300 Nm: (a) stator current; (b) torque; (c) FFT analysis result of the torque shows that over-modulation occurs in the TPFS inverter-fed DFIG drive if the rotor speed is reduced to 15 rpm.

The theoretical analysis is supported by the experimental result in Fig. 24 in that low frequency torque ripples are

produced at ω_m=15 rpm. This experimental result coincides well with the analysis in Section IV in that the TPFS inverter-fed DFIG drive is likely to operate in the over-modulation zone at low rotor speeds. According to (31), the DC bus voltage is set to 500 V, where the over-modulation is eliminated, as shown in Fig. 25. The experimental result shows that the conventional judgment of over-modulation using (24) cannot expose the effects of torque, capacitor voltage offset and rotor speed, thus demonstrating that it is not applicable for the proposed TPFS inverter-fed PMSM drive. To avoid torque ripples caused bythe over-modulation, the DC bus voltage should be properly selected using (31)

VI. CONCLUSION

This study gives sufficient insight into the causes and reduction of torque ripples in TPFS inverter-fed PMSM drives, and demonstrates that torque ripple reduction should be considered comprehensively from the perspective of capacitor voltage fluctuations, utilized SVM scheme, and linear modulation range. A very simple compensated modulation method is proposed in this study to directly calculate the duty ratios by introducing a non-orthogonal coordinate transformation, which can eliminate the 2nd-order torque ripples caused by capacitor voltage fluctuations. For the high-frequency torque ripple reduction, three commonly used SVM schemes are evaluated based on the criterion of RMS torque ripple values. It is clear that using the NVSVM, which employs the three nearest vectors to synthesize the reference vector, is able to reduce the high torque ripple effectively in the TPFS inverter-fed DFIG drive. Moreover, to investigate the accurate linear modulation range of the TPFS inverter-fed PMSM drive, an in-depth analysis is proposed based on the duty ratio equations. The analysis exposes that the linear modulation range is strongly influenced by the torque, capacitor voltage offset and rotor speed. Then, the appropriate DC bus voltage can be chosen to avoid low-frequency torque ripples caused by over-modulation. In addition, an improved capacitor voltage offset suppression method is proposed by implementing an adaptive notch filter, which guarantees the sufficient stability margin of the control loop at low rotor speeds. The suppression method can eliminate the capacitor voltage offset, whereby the full exploitation of the DC bus voltage can be ensured. The Simulink results demonstrate the effectiveness of the proposed comprehensive analysis and reduction of torque ripples in TPFS inverter-fed PMSM drives.

REFERENCES

[1] H. W. Van der Broeck and J. D. Van Wyk, "A Comparative Investigation of a Three-Phase Induction Machine Drive with a Component Minimized Voltage-Fed Inverter under Different Control Options," *IEEE Trans. Ind. Appl.*, vol. IA-20, no. 2, pp. 309-320, Mar. 1984.

[2] K. Gi-Taek and T. A. Lipo, "VSI-PWM rectifier/inverter system with a reduced switch count," *IEEE Trans. Ind. Appl.*, vol. 32, no. 6, pp. 1331-1337, Nov./Dec. 1996[3] F. Blaabjerg, S. Freysson, H. H. Hansen, and S. Hansen, "A new optimized space-vector modulation strategy for a component-minimized voltage source inverter," *IEEE Trans. Power Electron.*, vol. 12, no. 4, pp. 704-714, Jul. 1997.

[4] Z. Zeng, W. Zheng, R. Zhao, C. Zhu, and Q. Yuan, "Modeling, modulation, and control of the three-phase four-switch PWM rectifier under balanced voltage," *IEEE Trans. Power Electron.*, vol. 31, no. 7, pp. 4892-4905, Jul. 2016.

[5] Z. Zeng, W. Zheng and R. Zhao, "Space-vector-based hybrid PWM strategy for reduced DC-link capacitor current stress in the post-fault grid-connected three-phase rectifier," IEEE Trans. Power Electron., vol. 63, no. 8, pp. 4989-5000, Aug. 2016. 6] W. Wen, L. An, X. Xianyong, F. Lu, M. C. Thuyen, and L. Zhou, "Space vector pulse-width modulation algorithm and DC-side voltage control strategy of three-phase four-switch active power filters," *IET Power Electron.*, vol. 6, no. 1, pp. 125-135, Jan. 2013.

[7] Z. Zeng, W. Zheng, R. Zhao, C. Zhu, and Q. Yuan, "The comprehensive design and optimization of the post-fault grid-connected three-phase PWM rectifier," *IEEE Trans. Ind. Electron.*, vol. 63, no. 3, pp. 1629-1642, Mar. 2016.

[8] N. M. A. Freire and A. J. Marques Cardoso, "AFault-Tolerant Direct Controlled PMSG Drive for Wind Energy Conversion Systems," *IEEE Trans. Ind. Electron.*, vol. 61, no. 2, pp. 821-834, Feb. 2014.

[9] B. El Badsi, B. Bouzidi and A. Masmoudi, "DTC Scheme for a Four-Switch Inverter-Fed Induction Motor Emulating the Six-Switch Inverter Operation," *IEEE Trans. Power Electron.*, vol. 28, no. 7, pp. 3528-3538, Jul. 2013.

[10] M. Masmoudi, B. El Badsi and A. Masmoudi, "DTC of B4-inverter-fed BLDC motor drives with reduced torque ripple during sector-to-sector commutations," *IEEE Trans. Power Electron.*, vol. 29, no. 9, pp. 4855-4865, Sep. 2014

[11] Z. Dehong, Z. Jin and L. Yang, "Predictive torque control scheme for three-phase four-switch inverter-fed induction motor drives with dc-link voltages offset suppression," *IEEE Trans. Power Electron.*, vol. 30, no. 6, pp. 3309-3318, Jun. 2015. [12]J. Song-Manguelle, S. Schroder, T. Geyer, G. Ekemb, and J.-M. Nyobe-Yome, "Prediction of mechanical shaft failures due to pulsating torques of variable-frequency drives," *IEEE Trans. Ind. Appl.*, vol. 46, no. 5, pp. 1979–1988, Sep./Oct. 2010